A Comparison Between GA and PSO Algorithms in Training ANN to Predict the Refractive Index of Binary Liquid Solutions

Kamyar Movagharnejad* and Niusha Vafaei

Faculty of Chemical Engineering, Babol Noshirvani University of Technology, Babol, Iran

(Received: 08/24/2017, Revised: 09/14/2018, Accepted: 10/04/2018)
[DOI: 10.22059/JCHPE.2018.238595.1208]

Abstract

A total number of 1099 data points consisting of alcohol-alcohol, alcohol-alkane, alkane-alkane, alcohol-amine, and acid-acid binary solutions were collected from scientific literature to develop an appropriate artificial neural network (ANN), model. Temperature, molecular weight of the pure components, mole fraction of one component, and the structural groups of the components were used as input parameters of the network while the refractive index was selected as its output. The ANN was optimized once by the genetic algorithm (GA) and once again by the particle swarm optimization algorithm (PSO) in order to predict the refractive index of binary solutions. The optimal topology of the ANN-GA and ANN-PSO consisted of 13 and 16 neurons in the hidden layer, respectively. The results revealed that the ANN optimized with PSO had a better accuracy (MSE=0.003441 for test data) compared to the ANN optimized with GA (MSE=0.005117 for test data).

Keywords

Algorithm;
Artificial Neural Network;
Binary Liquid Mixture;
Genetic Multi-Layer Perceptron;
Particle Swarm Optimization;
Refractive Index

1. Introduction

The refractive index of a substance is defined as the ratio of the velocity of light in the vacuum to the velocity of light in the considered medium. This thermodynamic property depends on temperature and pressure for any pure fluid [1]. When the measurement of other thermodynamic properties is time-consuming, it is more convenient to measure the refractive index [2].

The refractive index of each material is a function of temperature but this function is different for each material. The refractive index may increase or decrease with temperature which depends on the medium.

The most general form of the Lorentz–Lorenz equation which describes the refractive index is as follows:

$$\frac{n_D^2-1}{n_D^2+2}=\frac{4\pi}{3}N\alpha \qquad (1)$$

where n_D is the refractive index, N is the number of molecules per unit volume, and α is the mean polarizability. This equation gives good es-

* Corresponding Author.
Tel.: 011-32334204
Email: k-movaghar@nit.ac.ir (K. Movagharnejad)

timates for liquids, solids and homogeneous solids.

For many gases the square of the refractive index is $n^2 \approx 1$, so this equation reduces to:

$$n^2 - 1 \approx 4\pi N\alpha \quad (2)$$

Or simply:

$$n - 1 \approx 2\pi N\alpha \quad (3)$$

This applies to gases at ordinary pressures. The refractive index of the gas may be expressed in terms of the molar refractivity as:

$$n \approx \sqrt{1 + \frac{3AP}{RT}} \quad (4)$$

where P is the pressure of the gas, R is the universal gas constant, and T is the absolute temperature. These parameters determine N which is the number density [3]. It is known that the refractive index for most glasses increases with temperature, while for plastic polymers, the opposite is true. The refractive index of water decreases with temperature. The decrease in the refractive index of most organic liquids with temperature is usually greater than water [4].

Refractive index has many applications, but the most important one may be the identification or concentration measurement of a specific substance. Generally, the refractive index is used to measure the concentration of solutes in aqueous solutions. For instance, in an aqueous sugar solution, the refractive index may be used to determine the sugar content (Brix degree), also it may be used to determine the drug concentration in the pharmaceutical industry. Another application of the refractive index may be the estimation of thermo-physical properties of hydrocarbons and petroleum mixtures [5].

Some empirical equations have been used to predict the refractive index. The relationship between refractive index, density and other physical properties of hydrocarbons investigated was by Lipkin and Martin:

$$n_D = \frac{69.878d - 0.4044Ad - 0.797A + 13.566}{5.543d - 0.746A + 126.683} \quad (5)$$

where n_D is the refractive index at 20 ℃ for the D line of sodium, d is the density at 20 ℃ and A is $-10^5 \times$ temperature coefficient of density (α), which is obtained from the approximate molecular weight [6].

The relation between refractive index with surface tension was introduced by Deetlefs for ionic liquids as below:

$$\sigma^{\frac{1}{4}} = \left(\frac{P}{R_m}\right)\left(\frac{n_D^2 - 1}{n_D^2 + 2}\right) \quad (6)$$

where n_D is the refractive index, P is the parachor, a surface-tension-weighted molar volume, and R_m is the molar refraction [7].

Sattari and his colleagues developed a based-group contribution method to predict the refractive indices of ionic liquids and they observed that the refractive index is a linear function of the temperature.

$$n_D = A + BT \quad (7)$$

$$A = 1.5082 + \sum_{i=1}^{k} n_{a,i}a_i \quad (8)$$

$$B = -1.4207 \times 10^{-4} + \sum_{i=1}^{k} n_{b,i}b_i \quad (9)$$

where n_i is the number of occurrences of the i^{th} functional group of anions and cations, k is the total number of different functional groups of the anions and cations, and a_i and b_i are the relevant coefficients of the i^{th} functional group [8].

There are numerous empirical equations based on experimental measurements for the prediction of the refractive index but these correlations have certain limitations. They usually include a large number of coefficients for each equation, require a separate equation for each temperature and they are not able to predict several parameters simultaneously. Recently, intelligent modeling techniques such as the artificial neural network (ANN) are successfully used to predict the different thermo-physical properties. The most important characteristic of the neural network models is their flexibility to predict the nonlinear behavior of chemical properties and their ability to estimate any function with high dimensional data. The mechanism of the ANN models is to construct relationships between the input and output data and predict the properties with reasonable accuracy [9, 10]. Recently, ANN models have been used to predict different thermodynamic properties such as viscosity, density, electrical conductivity, porosity, hardness and so on [11-18].

The method of evaluating properties using available experimental data to generate a model for predicting properties is called predictive computing [19]. Selection of an appropriate computer

algorithm such as the ANN is a vital step in this computational procedure.

Although the refractive index of some pure and a few mixtures was reported in the literature, these limited experimental data still cannot satisfy the requirements for their wide applications. Besides, experimental measurements are time-consuming and relatively expensive and are not always available, so estimation methods have been widely used instead of the rare experimental data [20].

The main purpose of this work is to develop a predictive model for the refractive index of binary mixtures. Specifically, it defines the best neural architecture using the ANN along with the parameters correlated with it, and it predicts the refractive index of the studied systems from the calculated empirical parameters.

For better response, the neural network trained by genetic (GA) and particle swarm optimization algorithm (PSO) independently.

2. Theory

In this section, the techniques of ANN, GA and PSO are briefly presented.

2.1. Artificial neural network algorithm (ANN)

The applicability of ANN in process industries and scientific research has been growing continuously in recent years [21]. Given adequate experimental data, the ANN model is able to approximate any continuous function with a satisfactory accuracy. The adequate performance of an ANN depends on several main elements. The first element is related to the collection of the input and output data. The second element is the type of the network architecture. Different network architectures may result in different estimations with varying degrees of accuracy. The third element is the model size and the problem complication. The model size and the problem complication have to be proportional to each other and the last element is related to the network training. In this paper like many other research papers in ANN modeling, the focus is on this last item [22].

ANN is a non-linear learning mathematical model that follows the human brain procedures. This technique is used in various scientific and engineering areas including prediction of physical and chemical properties. The input data is moved across any two successive layers and in each layer, the data is weighted and then passed to the next layer through a proper transfer function. In the training stage, the ANN revises the weights and biases of each neuron [19].

Gradient descent algorithms such as Back-Propagation (BP) method are used by many researchers in recent years. These researchers have included some of the advantages of these methods such as adequate implementations, better fine-tuning, and quicker convergence. However, some other researchers have listed the disadvantages of these methods such as involving in local minima and ill performances. So the common gradient search method is may be trapped in local optima. This is however not the case for Evolutionary Algorithms (EAs) which have better chances to reach the global optimal [22]. On the other hand, these algorithms are suitable for complicated problems [23]. Many different attempts have been tried by several researchers to solve this problem including imposing constraints on the search area, restarting training, adjusting training parameters, and reconstruction of the ANN architecture [24]. One of the most successful methods is to make use of EAs such as PSO, and GAs to train the ANNs. PSO or GA are global search algorithms and are more appropriate for local minima problems [25, 26].

When these algorithms are applied to neural networks, they find the best neural network architecture, optimizing the neural network learning parameters, and weights. In this way, emergence EAs and ANN may improve the predictive power of simple ANN, PSO or GA models [22].

2.2. Genetic algorithm (GA)

GA refers to a class of search algorithms that is known as Evolutionary Algorithms [27]. GA is based on the rule of "survival of fittest", referring to natural phenomena of genetic heredity. This algorithm operates on a population of individuals giving potential solutions to a certain problem. A single individual usually is affected by other neighboring individuals. Normally, the "fittest" individual has a greater chance to survive and multiply. This in turn heirs the good parental genetic information. Hence, after various genera-

tions, only the better individuals will survive. In general, GA may be applied to a wide range of optimization problems. GA was created to solve sequential decision processes but recently, it has been applied widely in both optimization and learning problems [28, 29]. The two main subjects in searching strategies for optimization problems are: exploiting the best solution and discovery of the search area [30, 31]. GA makes a balance between these two main subjects and also avoids the local minima. Fundamentally, the operation of weights evolution using GA belonged to the number of populations and generations. If these parameters were set nominal, the evolution may converge to a premature solution. However, the larger number of populations and generations would require longer convergence times [32].

The steps of GA to reach the optimum connection weights of ANN may be listed as follows:

At the first step, the primary population of random weights was generated to create the original ANN. Then the ANN was improved using the population weights by computing the training error. At the next section parents for genetic manipulation were selected and a new population of weights was constructed.

At the last section, the most appropriate population of weights was designated as the sequel of the performed GA, for the weights evolved using GA. The procedure may be terminated when the number of generation reaches a certain number [33].

Since the back propagation error algorithm is too slow, GA may be used to select the primary weight. In other words, by a combination of neural network with GA, the performance of the results may increase. In this research, in both training and testing data, GA was used to optimize the basic ANN behavior.

2.3. Particle swarm optimization (PSO)

PSO is a global optimization method introduced by Eberhart and Kennedy [33, 34]. The fundamental motivation of PSO algorithm was the social natural phenomena, such as flocks of birds and schools of fish in order to direct swarms of particles towards the most promising search area. PSO has shown a good performance in static optimization problems. In this method, a population of individuals is exploited to find the promising regions of the search area. In this study, we call the population a swarm and the individuals are called particles. Each particle in the swarm may be considered as a candidate solution. Each particle may move with a compatible velocity through the search area. These particles adjust their positions according to their own experience and also the experience of the neighboring particles. The mutual effect may be described as the fly of the particles towards the global minimum [35-37]. A predefined function describes the closeness of particles to the global minimum. In this research, a particle demonstrates the weight vector of ANNs, including biases. The dimension of the search area may be defined as the total number of weights and biases [22].

The PSO procedure can be described as follows. At first, a population size, locations, and velocities of factors, and the number of weights and biases were initialized. Then, the current best fitness attained by particle p was set as p_{best} .The p_{best} with the best value was set as g_{best} and stored. Subsequently, the agreeable optimization fitness function fp was evaluated for each particle as the Mean Square Error (MSE). Then, the evaluated fitness value fp of each particle was contrasted with its p_{best} value. If $fp < pbest$, then $pbest = fp$ and $best\,xp = xp$. where xp stands for the current coordinates of particle p, and the best xp stands for the coordinates corresponding to the best fitness of particle p. The objective function value was obtained for new locations of each particle. If a better position was obtained, $pbest$ value was replaced. As in Step 1, g_{best} value was selected among p_{best} values. If the new g_{best} value was better than the previous one, the g_{best} value was replaced. If $fp < gbest$ then $g_{best} = p$, where g_{best} is the particle having the overall best fitness over all particles in the swarm. The velocity and location of the particle may change due to the Eqs. 9 and 10, respectively [14, 19]. Then each particle p may fly according to Eq. 10. If you reach the maximum number of iterations, the procedure would be terminated; otherwise the procedure was looped to step 3 until convergence.

$$\mathrm{Vi} = \mathrm{wVi} - 1 + \mathrm{acc} * \mathrm{rand}\,() * (\mathrm{best\,xp} - \mathrm{xp}) + \mathrm{acc} * \mathrm{rand}\,() * (\mathrm{best\,xg}_{\mathrm{best}} - \mathrm{xp}) \quad (10)$$

where *acc* stands for the acceleration constant, and *rand* returns a uniform random number between 0 and 1.

$$xp = xpp + Vi \quad (11)$$

V_i is the current velocity, V_{i-1} is the former velocity, *xp* is the present particle location, *xpp* is the former particle location, and *i* is the particle index. In the last step the coordinates *bestxp* and *best xg* $_{best}$ are used to find the global minimum.

Similarly, the PSO algorithm was also applied to obtain the initial weights of the neural network. The inputs are the initial weights that should be calculated and the output is the summation of errors that should be minimized.

2.4. Data bank

Since this research is purely computational, all the data (experimental) needed for the calculations were taken from literature [38-46]. A total number of 1099 experimental data points for the refractive index were gathered in which the details are presented in Table 1, including the temperature range, mole fraction range, refractive index range, number of data points and the references.

Table 1. Name and specification of compounds

compound	T/K range	mole fraction	refractive index	data points	reference
methanol+n-pentane	298.15	0.0464-0.9734	1.3274-1.35359	10	[33]
methanol+n-hexane	298.15	0.0532-0.9771	1.32871-1.77118	11	[33]
methanol+n-heptane	298.15	0.0171-0.9765	1.32993-1.3838	9	[33]
methanol+n-octane	298.15	0.0367-0.9853	1.32962-1.39465	8	[33]
ethanol+n-pentane	298.15	0.0673-0.9174	1.3541-1.35823	10	[33]
ethanol+n-hexane	298.15	0.0569-0.9673	1.35988-1.37167	9	[33]
ethanol+n-heptane	298.15	0.0831-0.9744	1.36044-1.38382	9	[33]
ethanol+n-octane	298.15	0.0986-0.9773	1.3611-1.39295	9	[33]
1-propanol+n-pentane	298.15	0.0291-0.9586	1.35502-1.38162	10	[33]
1-propanol+n-hexane	298.15	0.1148-0.9594	1.37249-1.3823	9	[33]
1-propanol+n-heptane	298.15	0.0919-0.967	1.38398-1.38441	10	[33]
1-propanol+n-octane	298.15	0.1018-0.9677	1.385-1.39375	9	[33]
octane+ethanol	298.15	0.0686-0.9212	1.3641-1.3939	18	[34]
octane+propanol	298.15	0.0237-0.9245	1.3835-1.3943	18	[34]
octane+butanol	298.15	0.0453-0.9376	1.3948-1.397	15	[34]
octane+pentanol	298.15	0.0189-0.9457	1.3955-1.4075	17	[34]
octane+hexanol	298.15	0.0515-0.959	1.3956-1.4147	17	[34]
octane+heptanol	298.15	0.0616-0.9111	1.3971-1.4205	17	[34]
octane+octanol	298.15	0.0641-0.9635	1.3961-1.4257	16	[34]
pentane+hexane	298.15	0.1045-0.8997	1.3569-1.3715	9	[35]
pentane+heptane	298.15	0.1046-0.8929	1.359-1.3826	9	[35]
pentane+octane	298.15	0.1059-0.9035	1.361-1.3925	9	[35]
pentane+nonane	298.15	0.1995-0.904	1.3626-1.3975	8	[35]
pentane+decane	298.15	0.1031-0.9008	1.365-1.4068	9	[35]
pentane+undecane	298.15	0.0962-0.8967	1.3805-1.4152	9	[35]
pentane+dodecane	298.15	0.1094-0.8991	1.3684-1.4164	9	[35]
pentane+hexadecane	298.15	0.3099-0.9029	1.3747-1.4233	7	[35]
hexane+heptane	298.15	0.1059-0.8993	1.3745-1.3841	9	[35]
hexane+octane	298.15	0.1072-0.9018	1.3761-1.3937	9	[35]
hexane+nonane	298.15	0.1073-0.9035	1.3772-1.4009	9	[35]
hexane+decane	298.15	0.1074-0.9036	1.3788-1.4074	9	[35]
hexane+dodecane	298.15	0.1128-0.9037	1.381-1.4168	9	[35]
hexane+hexadecane	298.15	0.1046-0.9026	1.3864-1.4306	9	[35]
heptane+octane	298.15	0.1073-0.9012	1.3873-1.3945	9	[35]
heptane+nonane	298.15	0.1102-0.8996	1.3875-1.4021	9	[35]
heptane+decane	298.15	0.0985-0.903	1.3886-1.4086	9	[35]
heptane+undecane	298.15	0.1084-0.8998	1.3943-1.413	9	[35]

compound	T/K range	mole fraction	refractive index	data points	reference
heptane+dodecane	298.15	0.1076-0.9039	1.3907-1.4174	9	[35]
heptane+hexadecane	298.15	0.167-0.9019	1.3946-1.4316	9	[35]
octane+nonane	298.15	0.1092-0.9025	1.3963-1.4027	9	[35]
octane+decane	298.15	0.2142-0.9058	1.3968-1.4027	9	[35]
octane+undecane	298.15	0.1011-0.9039	1.3975-1.4132	9	[35]
octane+dodecane	298.15	0.1117-0.9048	1.3982-1.4177	9	[35]
octane+hexadecane	298.15	0.1039-0.9049	1.4015-1.4308	9	[35]
nonane+decane	298.15	0.1051-0.897	1.4043-1.4093	9	[35]
nonane+undecane	298.15	0.1034-0.9038	1.4045-1.4136	9	[35]
nonane+dodecane	298.15	0.0957-0.9023	1.4054-1.4183	9	[35]
nonane+hexadecane	298.15	0.1105-0.8988	1.4084-1.4323	9	[35]
decane+undecane	298.15	0.1074-0.9056	1.4105-1.4148	9	[35]
decane+dodecane	298.15	0.1071-0.9045	1.4115-1.419	9	[35]
decane+hexadecane	298.15	0.151-0.9041	1.417-1.4328	9	[35]
undecane+dodecane	298.15	0.106-0.9084	1.4156-1.4192	9	[35]
undecane+hexadecane	298.15	0.1095-0.9031	1.4182-1.4331	9	[35]
dodecane+hexadecane	298.15	0.1077-0.905	1.4218-1.4331	9	[35]
hexadecane+1-butanol	298.15-318.15	0.0903-0.9628	1.396-1.4347	30	[36]
hexadecane+1-pentanol	298.15	0.0831-0.9314	1.4101-1.4345	10	[36]
hexadecane+1-hexanol	298.15	0.0791-0.9184	1.4105-1.4347	10	[36]
hexadecane+1-heptanol	298.15	0.0893-0.9242	1.4123-1.4346	10	[36]
heptadecane+1-butanol	298.15	0.0867-0.9379	1.3996-1.4357	10	[36]
heptadecane+1-pentanol	298.15	0.1472-0.898	1.4103-1.4357	10	[36]
heptadecane+1-hexanol	298.15	0.0961-0.9107	1.4189-1.4356	10	[36]
heptadecane+1-heptanol	298.15	0.305-0.9194	1.4268-1.4357	8	[36]
methanol+2methyl,1butanol	298.15	0.0485-0.9503	1.33618-1.40702	19	[37]
ethanol+2methyl,1butanol	298.15	0.0486-0.9503	1.36358-1.40734	18	[37]
propanol+2methyl,1butanol	298.15	0.051-0.949	1.38483-1.40768	19	[38]
propanol+3methyl,1butanol	298.15	0.05-0.95	1.38458-1.40447	19	[38]
heptanoic acid+propanoic acid	293.15-313.15	0.0539-0.95	1.3816-1.4223	55	[39]
heptanoic acid+butanoic acid	293.15-313.15	0.0559-0.9575	1.392-1.4226	55	[39]
1-Propanol+ dicyclohexylamine	288.15-323.15	0.0527-0.9491	1.38876-1.48522	88	[40]
1-butanol+ dicyclohexylamine	288.15-323-15	0.0512-0.9493	1.39701-1.48502	88	[40]
1-pentanol+dicyclohexylamine	288.15-323.15	0.0525-0.9495	1.40539-1.48486	88	[40]

2.5. Criteria assessment of models

The statistical parameters such as the mean squared error (MSE) and the coefficient of determination (R^2) and the average absolute relation deviation (AARD) is applied for the performance assessment and to identify the accuracy of the developed ANN models which are defined as follows:

Mean squared errors:

$$\mathrm{MSE} = \frac{1}{\mathrm{N}}\sum_{\mathrm{i=1}}^{\mathrm{N}}(\left|\mathrm{y_{prd,i}} - \mathrm{y_{exp,i}}\right|)^2 \qquad (12)$$

Average absolute relative deviations:

$$\mathrm{AARD\%} = \frac{100}{\mathrm{N}}\sum_{\mathrm{i=1}}^{\mathrm{N}}\frac{\left|\mathrm{y_{prd,i}} - \mathrm{y_{exp,i}}\right|}{\mathrm{y_{exp,i}}} \qquad (13)$$

Squared correlation coefficients:

$$\mathrm{R^2} = 1 - \frac{\sum_{\mathrm{i=1}}^{\mathrm{N}}(\mathrm{y_{prd,i}} - \mathrm{y_{exp,i}})}{\sum_{\mathrm{i=1}}^{\mathrm{N}}(\mathrm{y_{prd,i}} - \mathrm{y_m})} \qquad (14)$$

where $y_{prd,i}$ is the predicted value using the ANN model, $y_{exp,i}$ is the experimental value, N is the number of data, and y_m is the average of the experimental value.

3. Results and Discussions

3.1. Model structure

The ANN model applied in this research consists of ten input nodes representing temperature, mole fractions, molecular weights and 6 functional groups of CH_3, CH_2, CH, OH, NH and COOH. The output is the only target, refractive index.

Before performing the ANN training stage, a data set is obtained from the literature [33-41]. There is a difference in magnitude and dimension of experimental data, therefore it should be normalized before being training stage. Manifold ANN structures were considered to choose the most accurate architecture. The optimal number of neurons was specified by trial and error.

The effectiveness of ANN in training stage must improve with augmenting the number of neurons, while the effectiveness of ANN in testing stage results in optimum value at an optimal number of hidden neurons. After training the ANN successfully, the trained network model was used to predict the testing data set and the comparison of the predicted and experimental data was carried out. The trained model was then assumed successful if the model would have given good outcomes for the testing data set. As mentioned above, the ANN training was started with 1 neuron in the hidden layer and piecemeal the neuron number increased.

The architecture consists of one input layer followed by a hidden layer and an output layer. Aside from temperature, the mole fraction of the first component and molecular weights, the input set consists of 6 functional groups of CH_3, CH_2, CH, OH, NH and COOH. The optimal number of neurons was determined according to the lowest AARD%. The optimal ANN-GA consisted of 13 neurons in the hidden layer and the optimal ANN-PSO consisted of 16 neurons in the hidden layer. Thus, the best ANN topology was attained as (10-13-1) for ANN-GA and (10-16-1) for ANN-PSO.

3.2. ANN-GA model

The combination of ANN and GA was used. This means that the weights of the neural network were determined using GA. First, the structure of the neural network should have been determined by the user. That was the number of neurons. Then, the neural network weights were determined by using a GA. The GA is capable to optimize and minimize an objective function, which here should be minimized, is the difference between the actual data and output data of a neural network. This means that, at any stage, weight coefficients were selected and neural network output was calculated, and its difference with the actual data was obtained, which in fact was the objective function value. In Fig. 2 the Objective function (MSE) is drawn by max generations.

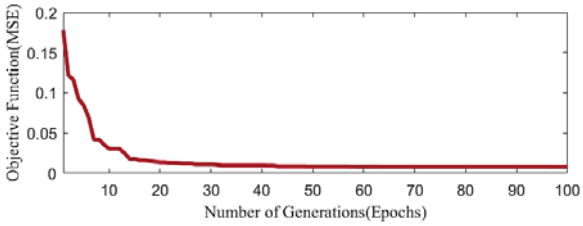

Figure 2. Objective function with the number of generations for ANN-GA model

We inserted 1099 refractive indices in the database, trained, validated and tested the network, and then, according to the output obtained after optimization of the weights by GA, the neural network is better trained. As a result, the refractive index that was predicted is very close to the actual refractive index. Figs. 3, 4 and 5 show the results of applying this algorithm for train and validation test data:

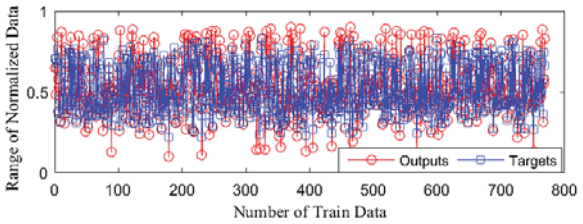

Figure 3. Experimental and Predicted Train Data for ANN-GA model

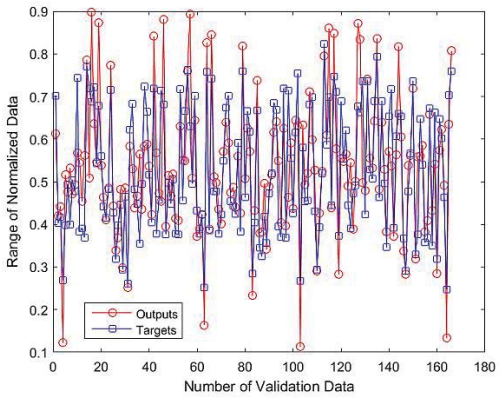

Figure 4. Experimental and Predicted Validation Data for ANN-GA model

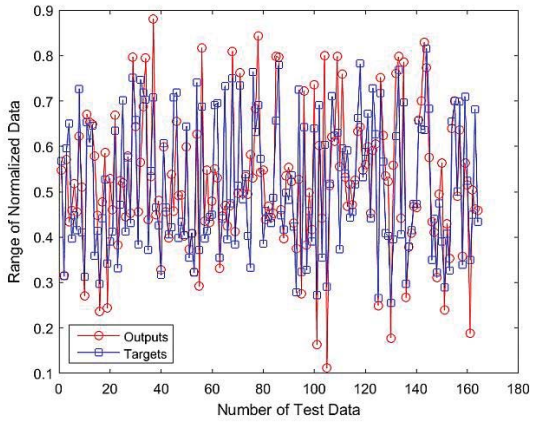

Figure 5. Experimental and Predicted Test Data for ANN-GA model

3.3. ANN-PSO

In this section, the particle swarm optimization algorithm was used to optimize the weights of the neural network to predict the refractive index of binary solutions. At this stage, 1099 refractive indices of the database were used. Figs. 6, 7 and 8 show that the actual data and the model predictions are in good agreement with each other. The results are given in the Tables 2 and 3.

Table 2. Results of prediction of binary solutions refractive indices using ANN-GA with 10-13-1 structure

Data-set Classification	MSE	AARD%	R^2
Train	0.0050181	8.2123	0.9091
Validation	0.0059107	2.4611	0.9851
Test	0.005117	1.4103	0.9884

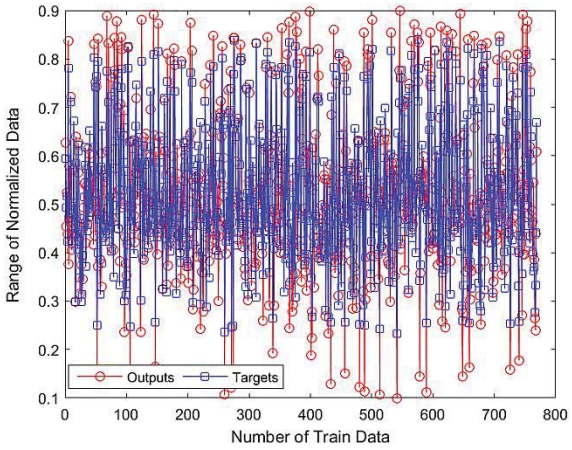

Figure 6. Experimental and Predicted Train Data for ANN-PSO model

Table 3. Results of prediction of binary solutions refractive indices using ANN-PSO with 10-16-1 structure

Data-set Classification	MSE	AARD%	R^2
Train	0.003836	7.9552	0.9944
Validation	0.003535	1.6643	0.9843
Test	0.003441	1.4024	0.9852

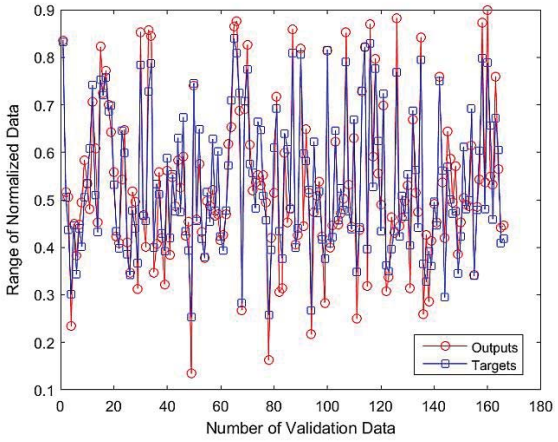

Figure 7. Experimental and Predicted Validation Data for ANN-PSO model

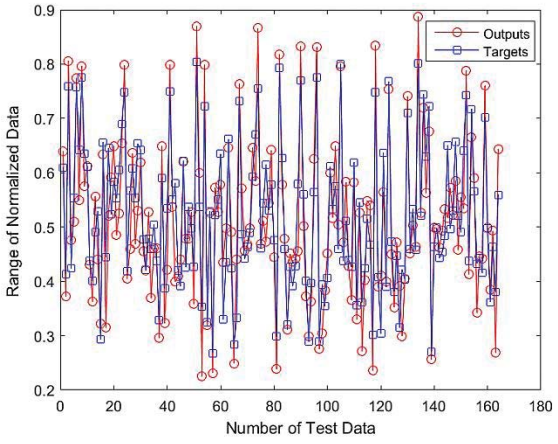

Figure 8. Experimental and Predicted Test Data for ANN-PSO model

4. Conclusions

An artificial neural network has been established to predict the refractive index of binary solutions including alcohol- alcohol, alcohol-alkane, alkane-alkane, alcohol-amine and acid-acid mixtures. In order to improve the performance of the neural network, the training process has been done by the genetic and particle swarm optimization algorithms independently, using 1099 data points

gathered from the published scientific literature. Temperature, the molecular weight of the pure components, the mole fraction of one component and 6 structural groups of the components were adapted as input parameters of the multi-layer perceptron neural network. The ANN-GA and ANN-PSO methodology have been compared with each other. The convergence performance and prediction accuracy of the PSO-based ANN are much better (MSE= 0.003441) than the GA based ANN (MSE=0.005117).

Acknowledgment

The authors acknowledge the funding support of the Babol Noshiravani University of Technology through Grant Program No. BNUT/370675/97.

References

[1] Riazi, M. R. and Roomi, Y. A. (2001). "Use of the Refractive Index in the Estimation of Thermophysical Properties of Hydrocarbons and Petroleum Mixtures." *Industrial & Engineering Chemistry Research*, Vol. 40, No. 8, pp. 1975-1984.

[2] Ali, A. and Tariq, T. (2008). "Deviations in refractive index parameters and applicability of mixing rules in binary mixtures of benzene +1, 2-dichloroethane at different temperatures." *Chemical Engineering Communications*, Vol. 195, No.1, pp. 43–56.

[3] Lorentz, A. H. (1881). "Ueber die Anwendung des Satzes vom Virial in der kinetischen Theorie der Gase." Wiedemanns Annalen (Annalen der Physik), Vol. 248, No. 1, pp. 127–136.

[4] Tropf., W. J., Thomas, M. E. and Harris, T. J. (1995). *Handbook of Optics*. 2nd ed. Vol. 2, Chapter 33, McGraw-Hill, New York.

[5] Koohyar F. J. (2013). "Refractive Index and Its Applications." *Journal of Thermodynamics & Catalysis*, Vol.4, No.2.

[6] Lipkin, M. R. and Martin, C. C. (1946), "Equation Relating Density, Refractive index, and Molecular Weight for Paraffins and Naphthenes." *Industrial and Engineering Chemistry*, vol. 18, No. 6. pp. 380-382.

[7] Deetlefs, M., Seddon, K.R. and Shara, M. (2006). "Predicting of Physical Properties of Ionic Liquids." *Physical Chemistry Chemical Physics*, Vol.8, No. 5, pp. 642-649.

[8] Sattari, M., Kamari, A., Mohammadi, A.H. and Ramjugernath, D. (2014). "A group contribution method for estimating the refractive indices of ionic liquids." *Molecular Liquids*, Vol. 200, Part B, pp. 410-415.

[9] Moosavi, M. and Soltani, N. (2013). "Prediction of hydrocarbon densities using an artificial neural network–group contribution method up to high temperatures and pressures." *Thermochimica Acta*, Vol. 556, pp. 89-96.

[10] Lashkarblooki, M., Hezave, A. Z., Al-Ajmi, A. M. and Ayatollahi, S. (2012). "Viscosity prediction of ternary mixtures containing ILs using multi-layer perceptron artificial neural network." *Fluid Phase Equilibria* Vol. 326, pp.15-20.

[11] Ozerdem, M. S. (2008). "Artificial neural network approach to predict the electrical conductivity and density of Ag–Ni binary alloys." *Journal of Materials Processing Technology*, Vol. 208, No. 1-3, pp. 470-476.

[12] Griffin, W. O. and Darsey, J. A. (2013). "Artificial neural network prediction indicators of density functional theory metal hydride models." *International Journal of Hydrogen Energy*, Vol. 38, No. 27, pp. 11920-11929.

[13] Hassan, A. M., Alrashdan, A., Hayajneh, M.T. and Mayyas, A.T. (2009). "Prediction of density, porosity and hardness in aluminum–copper-based composite materials using artificial neural network." *Journal of Materials Processing Technology*, Vol. 209, No. 2, pp. 894-899.

[14] Torkar, D., Novak, S. and Novak, F. (2008). "Apparent viscosity prediction of alumina–paraffin suspensions using artificial neural networks", *Journal of Materials Processing Technology*, Vol. 203, No. 1-3, pp. 208-215.

[15] Ghaderi, F., Ghaderi, A. H., Najafi, B. and Ghaderi, N. (2013). "Viscosity prediction by computational method and artificial neural network approach: The case of six refrigerants." *The Journal of Supercritical Fluids*, Vol. 81, pp. 67-78.

[16] Deosarkar, M. P. and Sathe, V. S. (2012). "Predicting effective viscosity of magnetite ore slurries by using artificial neural network." *Powder Technology*, Vol. 219, pp. 264-270.

[17] Salam, M., Al-Alawi, S. and Maqrashi, A. (2008). "Prediction of equivalent salt deposit density of contaminated glass plates using artificial neural networks." *Journal of Electrostatics*, Vol. 66, pp. 526-530.

[18] Ahmadi, S. H., Sepaskhah, A. R., Andersen, M.N., Plauborg, F., Jensen, C. R. and Hansen, S. (2014). "Modeling root length density of field grown potatoes under different irrigation strategies and soil textures using artificial neural networks." *Field Crops Research.* Vol. 162, pp. 99-107.

[19] Ghaedi, A. (2015). "Simultaneous prediction of the thermodynamic properties of aqueous solution of ethylene glycol monoethyl ether using artificial neural network." *Journal of Molecular Liquids*, Vol. 207, pp.327-333.

[20] Soriano, A. N., Ornedo-Ramos, K. F. P., Muriel, C. A. M., Adornado, A. P., Bungay, V. C., & Li, M. H. (2016). "Prediction of refractive index of binary solutions consisting of ionic liquids and alcohols (methanol or ethanol or 1-propanol) using artificial neural network", *Journal of the Taiwan Institute of Chemical Engineers*, Vol.65, pp. 83-90.

[21] Sexton, R. S., Dorsey, R. E. and Sikander, N.A. (2002). "Simultaneous optimization of neural network function and architecture algorithm." *Decision Support Systems*, pp. 1034-1047.

[22] Braik M., Sheta A. and Arieqat A. (2008). "A comparison between GAs and PSO in training ANN to model the TE chemical process reactor." In *AISB 2008 Convention communication, interaction and social intelligence*, Vol. 11, p. 24-30.

[23] Fogel, D. B. (1994). "An introduction to simulated evolutionary optimization." *IEEE Transactions on Neural Networks*, Vol. 5, No. 1, pp. 3-14.

[24] Huang, Y. (2009). "Advances in Artificial Neural Networks – Methodological

Development and Application", *Algorithms.* Vol. 2, No. 3, pp.973-1007.

[25] Abbass, H. A., Sarker, R. and Newton, C. (2001). "PDE: A Pareto-frontier Differential Evolution Approach for Multi-objective Optimization Problems." in *Proceedings of the Congress on Evolutionary Computation 2001 (CEC'2001),* Vol. 2, pp. 971–978, Piscataway, New Jersey, IEEE Service Center.

[26] Kiran, R., Jetti, S. R. and Venayagamoorthy, G. K. (2006). 'Online training of generalized neuron with particle swarm optimization', in International Joint Conference on Neural Networks, IJCNN 06, Vancouver, BC, Canada, pp. 5088–5095. IEEE, (2006).

[27] Choenauer, M. and Michalewicz, Z. (1997). "Evolutionary computation control and cybernetics." *Proceedings of the IEEE*, Vol. 26, No. 3, pp. 307–338.

[28] Sit, C. W. (2005). "Application of Artificial Neural Network-Genetic Algorithm in Inferential Estimation and Control of a Distillation Column", ME thesis, Faculty of Chemical and Natural Resources Engineering, Universiti Teknologi Malaysia.

[29] Sheta, A. and Turabieh, H. (2006). "A comparison between genetic algorithms and sequential quadratic programming in solving constrained optimization problems", *ICGST International Journal on Artificial Intelligence and Machine Learning*, Vol. 6, No. 1, pp. 67–74.

[30] Gen, M. and Cheng, R. (1997). *Genetic Algorithms and Engineering Design*, John Wiley & Son, Inc., Hoboken.

[31] Sheta, A., Turabieh, H. and Vasant, P. (2007). "Hybrid optimization genetic algorithms (HOGA) with interactive evolution to solve constraint optimization problems." *International Journal of Computational Science*, Vol.1, No. 4, pp. 395–406.

[32] Sheta A. and Eghneem, K. (2007). "Training artificial neural networks using genetic algorithms to predict the price of the general index for Amman stock exchange", in Midwest Artificial Intelligence and Cognitive Science Conference, DePaul University, Chicago, IL, USA, Vol. 92, pp. 7–13.

[33] Kennedy, J. and Eberhart, R. C. (1995). "Particle swarm optimization', Proceedings of IEEE International Conference on Neural Networks (Perth, Australia), IEEE Service Center, Piscataway, NJ, Vol. 5, No. 3, pp. 1942–1948.

[34] Kennedy, J., Eberhart, R. C. and Shi, Y. (2001). *Swarm Intelligence*, Morgan Kaufmann Publishers, San Francisco.

[35] Kiran, R., Jetti, S. R. and Venayagamoorthy G. K. (2006). "Online training of generalized neuron with particle swarm optimization", in Interna-

tional Joint Conference on Neural Networks, IJCNN 06, Vancouver, BC, Canada, pp. 5088–5095. IEEE.

[36] Richer, T.J. and Blackwell, T.M. (2006). "When is a swarm necessary?", in Proceedings of the 2006 IEEE Congress on Evolutionary Computation, eds., Gary G. Yen, Simon M. Lucas, Gary Fogel, Graham Kendall, Ralf Salomon, Byoung-Tak Zhang, Carlos A. Coello, and Thomas Philip Runarsson, pp. 1469–1476, Vancouver, BC, Canada, IEEE Press.

[37] Kwok, N., Liu, D. and Tan, K. (2006). "An empirical study on the setting of control coefficient in particle swarm optimization", in Proceedings of IEEE Congress on Evolutionary Computation (CEC 2006), Vancouver, BC, Canada, pp. 3165–3172, Vancouver, BC, Canada, IEEE Press.

[38] Orge, B., Iglesias, M., Rodriguez, A., Canosa, J. M. and Tojo. J. (1997) "Mixing properties of (methanol, ethanol, or 1-propanol) with (n-pentane, n-hexane, n-heptane and n-octane) at 298.15 K." *Fluid Phase Equilibria*, Vol. 133, No. 1-2, pp. 213-227.

[39] Segade., L., de Liano, J. J., Domınguez-Prez, M., Oscar, C., Cabanas, M. and Jimenez. E. (2003). "Density, Surface Tension, and Refractive Index of Octane + 1-Alkanol Mixtures at T = 298.15 K." *Journal of Chemical & Engineering Data*, Vol. 48, No. 5, pp.1251-1255.

[40] Aucejo, A., Burguet, A. C., Munoz, R. and Marques, J.L. (1995). "Densities, Viscosities, and Refractive Indices of Some n-Alkane Binary Liquid Systems at 298.15 K." *Journal of Chemical and Engineering Data*, Vol. 40, No. 1, pp. 141-147.

[41] Mehra, R. (2003). "Application of refractive index mixing rules in binary systems of hexadecane and heptadecane with *n*-alkanols at different temperatures." *Journal of Chemical Sciences.* Vol. 115, No. 2, pp. 147–154.

[42] Resa, J. M., Gonzalez, C. and Goenaga, J. M. (2005). "Density, Refractive Index, Speed of Sound at 298.15 K, and Vapor-Liquid Equilibria at 101.3 kPa for Binary Mixtures of Methanol + 2-Methyl-1-butanol and Ethanol + 2-Methyl-1-butanol." *Journal of Chemical & Engineering Data*, Vol. 50, No. 5, pp.1570-1575.

[43] Resa, J.M., Gonzalez, C. and Goenaga, J. M. (2006). "Density, Refractive Index, Speed of Sound at 298.15 K, and Vapor-Liquid Equilibria at 101.3 kPa for Binary Mixtures of Propanol + 2-Methyl-1-butanol and Propanol + 3-Methyl-1-butanol." *Journal of Chemical & Engineering Data*, Vol. 51, Vol. 1, pp. 73-78.

[44] Bahadur, I., Naidoo, P., Singh, S., Ramjugernath, D. and Deenadayalu, N. (2014). "Effect of temperature on density, sound velocity, refractive index and their derived properties for the binary systems (heptanoic acid + propanoic or butanoic acids)", *The Journal of Chemical Thermodynamics*, Vol. 78 pp. 7–15.

[45] Kijevcanin, M. L., Radovic, I. R., Djordjevic, B. D., Tasic, A.Z. and Serbanovic, S. P. (2011). "Experimental determination and modeling of densities and refractive indices of the binary systems alcohol + dicyclohexylamine at T = (288.15–323.15) K." *Themochimica Acta* Vol. 525, No. 1, pp.114– 128.

[46] Poling, B. E., Prausnitz, J. M. and O'Connell, J. (2001). *The Properties of Gases and Liquids*, 5th edition. Mcgraw-hill. New York. pp. 723-73.